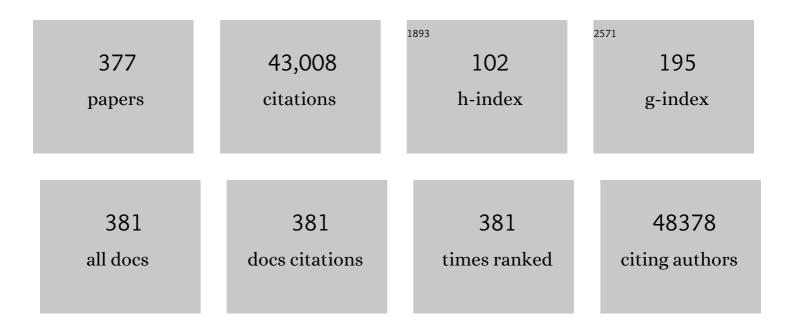
List of Publications by Year in descending order

Source: https://exaly.com/author-pdf/719205/publications.pdf Version: 2024-02-01



DENC CHEN

#	Article	IF	CITATIONS
1	Glowing Graphene Quantum Dots and Carbon Dots: Properties, Syntheses, and Biological Applications. Small, 2015, 11, 1620-1636.	10.0	1,770
2	Biological and chemical sensors based on graphene materials. Chemical Society Reviews, 2012, 41, 2283-2307.	38.1	1,591
3	Heteroatom-doped graphene materials: syntheses, properties and applications. Chemical Society Reviews, 2014, 43, 7067-7098.	38.1	1,547
4	3D Graphene–Cobalt Oxide Electrode for High-Performance Supercapacitor and Enzymeless Glucose Detection. ACS Nano, 2012, 6, 3206-3213.	14.6	1,510
5	In Situ Synthesis of Metal Nanoparticles on Single-Layer Graphene Oxide and Reduced Graphene Oxide Surfaces. Journal of Physical Chemistry C, 2009, 113, 10842-10846.	3.1	702
6	Solution-processable 2D semiconductors for high-performance large-area electronics. Nature, 2018, 562, 254-258.	27.8	644
7	Recent Advances on Graphene Quantum Dots: From Chemistry and Physics to Applications. Advanced Materials, 2019, 31, e1808283.	21.0	603
8	Centimeter-Long and Large-Scale Micropatterns of Reduced Graphene Oxide Films: Fabrication and Sensing Applications. ACS Nano, 2010, 4, 3201-3208.	14.6	571
9	In Situ Growth of 2D Perovskite Capping Layer for Stable and Efficient Perovskite Solar Cells. Advanced Functional Materials, 2018, 28, 1706923.	14.9	543
10	Doping Single‣ayer Graphene with Aromatic Molecules. Small, 2009, 5, 1422-1426.	10.0	537
11	Revealing the tunable photoluminescence properties of graphene quantum dots. Journal of Materials Chemistry C, 2014, 2, 6954-6960.	5.5	530
12	Macroporous and Monolithic Anode Based on Polyaniline Hybridized Three-Dimensional Graphene for High-Performance Microbial Fuel Cells. ACS Nano, 2012, 6, 2394-2400.	14.6	520
13	Robust epitaxial growth of two-dimensional heterostructures, multiheterostructures, and superlattices. Science, 2017, 357, 788-792.	12.6	518
14	Electrical Detection of DNA Hybridization with Singleâ€Base Specificity Using Transistors Based on CVDâ€Grown Graphene Sheets. Advanced Materials, 2010, 22, 1649-1653.	21.0	516
15	Surface Modified Ti ₃ C ₂ MXene Nanosheets for Tumor Targeting Photothermal/Photodynamic/Chemo Synergistic Therapy. ACS Applied Materials & Interfaces, 2017, 9, 40077-40086.	8.0	491
16	Superhydrophobic and superoleophilic hybrid foam of graphene and carbon nanotube for selective removal of oils or organic solvents from the surface of water. Chemical Communications, 2012, 48, 10660.	4.1	471
17	Facile Synthesis of Graphene Quantum Dots from 3D Graphene and their Application for Fe ³⁺ Sensing. Advanced Functional Materials, 2014, 24, 3021-3026.	14.9	446
18	One-Pot Synthesis of Carbon-Coated SnO ₂ Nanocolloids with Improved Reversible Lithium Storage Properties. Chemistry of Materials, 2009, 21, 2868-2874.	6.7	421

#	Article	IF	CITATIONS
19	Ultralong Phosphorescence of Waterâ€Soluble Organic Nanoparticles for In Vivo Afterglow Imaging. Advanced Materials, 2017, 29, 1606665.	21.0	419
20	New BiVO ₄ Dual Photoanodes with Enriched Oxygen Vacancies for Efficient Solarâ€Driven Water Splitting. Advanced Materials, 2018, 30, e1800486.	21.0	414
21	Ligand-assisted cation-exchange engineering for high-efficiency colloidal Cs1â^'xFAxPbI3 quantum dot solar cells with reduced phase segregation. Nature Energy, 2020, 5, 79-88.	39.5	412
22	Nanoelectronic biosensors based on CVD grown graphene. Nanoscale, 2010, 2, 1485.	5.6	408
23	Quantum dots derived from two-dimensional materials and their applications for catalysis and energy. Chemical Society Reviews, 2016, 45, 2239-2262.	38.1	391
24	Atomic Layer Deposition to Fine-Tune the Surface Properties and Diameters of Fabricated Nanopores. Nano Letters, 2004, 4, 1333-1337.	9.1	385
25	An Electrochemically Treated BiVO ₄ Photoanode for Efficient Photoelectrochemical Water Splitting. Angewandte Chemie - International Edition, 2017, 56, 8500-8504.	13.8	369
26	Strategies for enhancing the sensitivity of plasmonic nanosensors. Nano Today, 2015, 10, 213-239.	11.9	356
27	Boosting the Photocatalytic Ability of Cu ₂ 0 Nanowires for CO ₂ Conversion by MXene Quantum Dots. Advanced Functional Materials, 2019, 29, 1806500.	14.9	354
28	Graphene-based biosensors for detection of bacteria and their metabolic activities. Journal of Materials Chemistry, 2011, 21, 12358.	6.7	343
29	Probing Single DNA Molecule Transport Using Fabricated Nanopores. Nano Letters, 2004, 4, 2293-2298.	9.1	341
30	Systematic Bandgap Engineering of Graphene Quantum Dots and Applications for Photocatalytic Water Splitting and CO ₂ Reduction. ACS Nano, 2018, 12, 3523-3532.	14.6	341
31	Hybrid Fibers Made of Molybdenum Disulfide, Reduced Graphene Oxide, and Multiâ€Walled Carbon Nanotubes for Solid‣tate, Flexible, Asymmetric Supercapacitors. Angewandte Chemie - International Edition, 2015, 54, 4651-4656.	13.8	334
32	Transparent, Flexible, All-Reduced Graphene Oxide Thin Film Transistors. ACS Nano, 2011, 5, 5038-5044.	14.6	305
33	A Swellable Microneedle Patch to Rapidly Extract Skin Interstitial Fluid for Timely Metabolic Analysis. Advanced Materials, 2017, 29, 1702243.	21.0	303
34	Interfacing Live Cells with Nanocarbon Substrates. Langmuir, 2010, 26, 2244-2247.	3.5	301
35	Oxygenic Hybrid Semiconducting Nanoparticles for Enhanced Photodynamic Therapy. Nano Letters, 2018, 18, 586-594.	9.1	294
36	3D Graphene Foam as a Monolithic and Macroporous Carbon Electrode for Electrochemical Sensing. ACS Applied Materials & Interfaces, 2012, 4, 3129-3133.	8.0	292

#	Article	IF	CITATIONS
37	Addressing Toxicity of Lead: Progress and Applications of Lowâ€Toxic Metal Halide Perovskites and Their Derivatives. Advanced Energy Materials, 2017, 7, 1602512.	19.5	290
38	Hybrid structure of zinc oxide nanorods and three dimensional graphene foam for supercapacitor and electrochemical sensor applications. RSC Advances, 2012, 2, 4364.	3.6	285
39	Rare-Earth Single-Atom La–N Charge-Transfer Bridge on Carbon Nitride for Highly Efficient and Selective Photocatalytic CO ₂ Reduction. ACS Nano, 2020, 14, 15841-15852.	14.6	283
40	Electrical Detection of Metal Ions Using Field-Effect Transistors Based on Micropatterned Reduced Graphene Oxide Films. ACS Nano, 2011, 5, 1990-1994.	14.6	279
41	Understanding the Roles of Oxygen Vacancies in Hematiteâ€Based Photoelectrochemical Processes. Angewandte Chemie - International Edition, 2019, 58, 1030-1034.	13.8	268
42	Nitrogen defect structure and NO+ intermediate promoted photocatalytic NO removal on H2 treated g-C3N4. Chemical Engineering Journal, 2020, 379, 122282.	12.7	260
43	Recent progress in the development of near-infrared organic photothermal and photodynamic nanotherapeutics. Biomaterials Science, 2018, 6, 746-765.	5.4	250
44	Regulating Near-Infrared Photodynamic Properties of Semiconducting Polymer Nanotheranostics for Optimized Cancer Therapy. ACS Nano, 2017, 11, 8998-9009.	14.6	239
45	In Situ Formation of Oxygen Vacancies Achieving Nearâ€Complete Charge Separation in Planar BiVO ₄ Photoanodes. Advanced Materials, 2020, 32, e2001385.	21.0	236
46	Graphene Quantum Dots as Universal Fluorophores and Their Use in Revealing Regulated Trafficking of Insulin Receptors in Adipocytes. ACS Nano, 2013, 7, 6278-6286.	14.6	229
47	Organic Dye Based Nanoparticles for Cancer Phototheranostics. Small, 2018, 14, e1704247.	10.0	226
48	Observation of Strong Interlayer Coupling in MoS ₂ /WS ₂ Heterostructures. Advanced Materials, 2016, 28, 1950-1956.	21.0	225
49	Symmetry Breaking of Graphene Monolayers by Molecular Decoration. Physical Review Letters, 2009, 102, 135501.	7.8	224
50	Graphene-wrapped TiO2 hollow structures with enhanced lithium storage capabilities. Nanoscale, 2011, 3, 2158.	5.6	223
51	Activatable Photoacoustic Nanoprobes for In Vivo Ratiometric Imaging of Peroxynitrite. Advanced Materials, 2017, 29, 1604764.	21.0	220
52	Grapheneâ€Contacted Ultrashort Channel Monolayer MoS ₂ Transistors. Advanced Materials, 2017, 29, 1702522.	21.0	218
53	Metal–organic framework derived CoSe2 nanoparticles anchored on carbon fibers as bifunctional electrocatalysts for efficient overall water splitting. Nano Research, 2016, 9, 2234-2243.	10.4	215
54	Synthesis of a MnO2–graphene foam hybrid with controlled MnO2 particle shape and its use as a supercapacitor electrode. Carbon, 2012, 50, 4865-4870.	10.3	214

#	Article	IF	CITATIONS
55	Electrodeposited Pt on three-dimensional interconnected graphene as a free-standing electrode for fuel cell application. Journal of Materials Chemistry, 2012, 22, 5286.	6.7	210
56	Van der Waals epitaxial growth of air-stable CrSe2 nanosheets with thickness-tunable magnetic order. Nature Materials, 2021, 20, 818-825.	27.5	206
57	De Novo Reconstruction of Adipose Tissue Transcriptomes Reveals Long Non-coding RNA Regulators of Brown Adipocyte Development. Cell Metabolism, 2015, 21, 764-776.	16.2	201
58	Graphene quantum dots functionalized gold nanoparticles for sensitive electrochemical detection of heavy metal ions. Electrochimica Acta, 2015, 172, 7-11.	5.2	200
59	Synthesis of graphene–carbon nanotube hybrid foam and its use as a novel three-dimensional electrode for electrochemical sensing. Journal of Materials Chemistry, 2012, 22, 17044.	6.7	197
60	Bi metal prevents the deactivation of oxygen vacancies in Bi2O2CO3 for stable and efficient photocatalytic NO abatement. Applied Catalysis B: Environmental, 2020, 264, 118545.	20.2	197
61	Label-free, electrochemical detection of methicillin-resistant staphylococcus aureus DNA with reduced graphene oxide-modified electrodes. Biosensors and Bioelectronics, 2011, 26, 3881-3886.	10.1	191
62	Real-time DNA detection using Pt nanoparticle-decorated reduced graphene oxide field-effect transistors. Nanoscale, 2012, 4, 293-297.	5.6	185
63	Synthesis of Ultrathin Metallic MTe ₂ (M = V, Nb, Ta) Single rystalline Nanoplates. Advanced Materials, 2018, 30, e1801043.	21.0	183
64	One-step growth of graphene–carbon nanotube hybrid materials by chemical vapor deposition. Carbon, 2011, 49, 2944-2949.	10.3	182
65	MOF-directed templating synthesis of a porous multicomponent dodecahedron with hollow interiors for enhanced lithium-ion battery anodes. Journal of Materials Chemistry A, 2015, 3, 8483-8488.	10.3	178
66	Ultra-large single-layer graphene obtained from solution chemical reduction and its electrical properties. Physical Chemistry Chemical Physics, 2010, 12, 2164.	2.8	176
67	Free-standing electrochemical electrode based on Ni(OH) ₂ /3D graphene foam for nonenzymatic glucose detection. Nanoscale, 2014, 6, 7424-7429.	5.6	174
68	Nitrogen and phosphorus co-doped graphene quantum dots: synthesis from adenosine triphosphate, optical properties, and cellular imaging. Nanoscale, 2015, 7, 8159-8165.	5.6	174
69	Effective doping of single-layer graphene from underlying <mml:math xmlns:mml="http://www.w3.org/1998/Math/MathML" display="inline" > <mml:mrow> <mml:mrow> <mml:mtext> SiO </mml:mtext> </mml:mrow> <mml:mn> Physical Review B. 2009. 79</mml:mn></mml:mrow></mml:math 	2< <mark>/</mark> mml:m	ın>
70	RGD-Peptide Functionalized Graphene Biomimetic Live-Cell Sensor for Real-Time Detection of Nitric Oxide Molecules. ACS Nano, 2012, 6, 6944-6951.	14.6	172
71	pH-Triggered and Enhanced Simultaneous Photodynamic and Photothermal Therapy Guided by Photoacoustic and Photothermal Imaging. Chemistry of Materials, 2017, 29, 5216-5224.	6.7	170
72	Layer-by-layer printing of laminated graphene-based interdigitated microelectrodes for flexible planar micro-supercapacitors. Electrochemistry Communications, 2015, 51, 33-36.	4.7	169

#	Article	IF	CITATIONS
73	Growth of large-sized graphene thin-films by liquid precursor-based chemical vapor deposition under atmospheric pressure. Carbon, 2011, 49, 3672-3678.	10.3	158
74	A graphene–cobalt oxide based needle electrode for non-enzymatic glucose detection in micro-droplets. Chemical Communications, 2012, 48, 6490.	4.1	155
75	Using oxidation to increase the electrical conductivity of carbon nanotube electrodes. Carbon, 2009, 47, 1867-1870.	10.3	152
76	Interfacing Glycosylated Carbonâ€Nanotubeâ€Network Devices with Living Cells to Detect Dynamic Secretion of Biomolecules. Angewandte Chemie - International Edition, 2009, 48, 2723-2726.	13.8	148
77	Broadband tunable liquid crystal terahertz waveplates driven with porous graphene electrodes. Light: Science and Applications, 2015, 4, e253-e253.	16.6	148
78	Thickness-Tunable Synthesis of Ultrathin Type-II Dirac Semimetal PtTe ₂ Single Crystals and Their Thickness-Dependent Electronic Properties. Nano Letters, 2018, 18, 3523-3529.	9.1	147
79	Ultrasensitive Profiling of Metabolites Using Tyramine-Functionalized Graphene Quantum Dots. ACS Nano, 2016, 10, 3622-3629.	14.6	145
80	Graphene quantum dot engineered nickel-cobalt phosphide as highly efficient bifunctional catalyst for overall water splitting. Nano Energy, 2018, 48, 284-291.	16.0	143
81	Thermally Induced Graphene Rotation on Hexagonal Boron Nitride. Physical Review Letters, 2016, 116, 126101.	7.8	142
82	A hierarchically structured composite of Mn ₃ O ₄ /3D graphene foam for flexible nonenzymatic biosensors. Journal of Materials Chemistry B, 2013, 1, 110-115.	5.8	137
83	Liquid-phase sintering of lead halide perovskites and metal-organic framework glasses. Science, 2021, 374, 621-625.	12.6	137
84	Three-Dimensional Graphene-Carbon Nanotube Hybrid for High-Performance Enzymatic Biofuel Cells. ACS Applied Materials & Interfaces, 2014, 6, 3387-3393.	8.0	136
85	Interconnected Tin Disulfide Nanosheets Grown on Graphene for Li-Ion Storage and Photocatalytic Applications. ACS Applied Materials & amp; Interfaces, 2013, 5, 12073-12082.	8.0	135
86	Graphene supported Sn–Sb@carbon core-shell particles as a superior anode for lithium ion batteries. Electrochemistry Communications, 2010, 12, 1302-1306.	4.7	132
87	Chemical synthesis of two-dimensional atomic crystals, heterostructures and superlattices. Chemical Society Reviews, 2018, 47, 3129-3151.	38.1	132
88	Digitalizing Selfâ€Assembled Chiral Superstructures for Optical Vortex Processing. Advanced Materials, 2018, 30, 1705865.	21.0	131
89	The formation of a carbon nanotube–graphene oxide core–shell structure and its possible applications. Carbon, 2011, 49, 5071-5078.	10.3	130
90	Nanochannel-Confined Graphene Quantum Dots for Ultrasensitive Electrochemical Analysis of Complex Samples. ACS Nano, 2018, 12, 12673-12681.	14.6	129

#	Article	IF	CITATIONS
91	Quantum Dots with Phenylboronic Acid Tags for Specific Labeling of Sialic Acids on Living Cells. Analytical Chemistry, 2011, 83, 1124-1130.	6.5	128
92	Enhanced perovskite electronic properties via a modified lead(<scp>ii</scp>) chloride Lewis acid–base adduct and their effect in high-efficiency perovskite solar cells. Journal of Materials Chemistry A, 2017, 5, 5195-5203.	10.3	128
93	Surface Chemistry Engineering of Perovskite Quantum Dots: Strategies, Applications, and Perspectives. Advanced Materials, 2022, 34, e2105958.	21.0	128
94	Supercapacitor electrode based on three-dimensional graphene–polyaniline hybrid. Materials Chemistry and Physics, 2012, 134, 576-580.	4.0	125
95	Liquidâ€Crystalâ€Mediated Geometric Phase: From Transmissive to Broadband Reflective Planar Optics. Advanced Materials, 2020, 32, e1903665.	21.0	124
96	Carbon nanotubes grown in situ on graphene nanosheets as superior anodes for Li-ion batteries. Nanoscale, 2011, 3, 4323.	5.6	119
97	Fabrication of Ultralong Hybrid Microfibers from Nanosheets of Reduced Graphene Oxide and Transitionâ€Metal Dichalcogenides and their Application as Supercapacitors. Angewandte Chemie - International Edition, 2014, 53, 12576-12580.	13.8	119
98	Multilayered semiconducting polymer nanoparticles with enhanced NIR fluorescence for molecular imaging in cells, zebrafish and mice. Chemical Science, 2016, 7, 5118-5125.	7.4	113
99	Non-enzymatic detection of hydrogen peroxide using a functionalized three-dimensional graphene electrode. Electrochemistry Communications, 2013, 26, 81-84.	4.7	109
100	Polydopamine-Enabled Approach toward Tailored Plasmonic Nanogapped Nanoparticles: From Nanogap Engineering to Multifunctionality. ACS Nano, 2016, 10, 11066-11075.	14.6	109
101	Synergistic effects of crystal structure and oxygen vacancy on Bi2O3 polymorphs: intermediates activation, photocatalytic reaction efficiency, and conversion pathway. Science Bulletin, 2020, 65, 467-476.	9.0	108
102	Arbitrary and reconfigurable optical vortex generation: a high-efficiency technique using director-varying liquid crystal fork gratings. Photonics Research, 2015, 3, 133.	7.0	106
103	Facile and scalable preparation of highly luminescent N,S co-doped graphene quantum dots and their application for parallel detection of multiple metal ions. Journal of Materials Chemistry B, 2017, 5, 6593-6600.	5.8	106
104	Chirality invertible superstructure mediated active planar optics. Nature Communications, 2019, 10, 2518.	12.8	106
105	Directional electron delivery and enhanced reactants activation enable efficient photocatalytic air purification on amorphous carbon nitride co-functionalized with O/La. Applied Catalysis B: Environmental, 2019, 242, 19-30.	20.2	103
106	Phase-controlled synthesis of α-NiS nanoparticles confined in carbon nanorods for High Performance Supercapacitors. Scientific Reports, 2014, 4, 7054.	3.3	101
107	Generation of arbitrary vector beams with liquid crystal polarization converters and vector-photoaligned q-plates. Applied Physics Letters, 2015, 107, .	3.3	100
108	van der Waals Heterojunction between a Bottom-Up Grown Doped Graphene Quantum Dot and Graphene for Photoelectrochemical Water Splitting. ACS Nano, 2020, 14, 1185-1195.	14.6	100

#	Article	IF	CITATIONS
109	Achieving stable and efficient water oxidation by incorporating NiFe layered double hydroxide nanoparticles into aligned carbon nanotubes. Nanoscale Horizons, 2016, 1, 156-160.	8.0	99
110	Unraveling the mechanism of binary channel reactions in photocatalytic formaldehyde decomposition for promoted mineralization. Applied Catalysis B: Environmental, 2020, 260, 118130.	20.2	99
111	CMOS ompatible Nanowire Sensor Arrays for Detection of Cellular Bioelectricity. Small, 2009, 5, 208-212.	10.0	98
112	Progress and Perspective in Lowâ€Dimensional Metal Halide Perovskites for Optoelectronic Applications. Solar Rrl, 2018, 2, 1700186.	5.8	98
113	Comparison of biochemical effects of statins and fish oil in brain: The battle of the titans. Brain Research Reviews, 2007, 56, 443-471.	9.0	97
114	Ferritin-Templated Synthesis and Self-Assembly of Pt Nanoparticles on a Monolithic Porous Graphene Network for Electrocatalysis in Fuel Cells. ACS Applied Materials & Interfaces, 2013, 5, 782-787.	8.0	96
115	An aza-BODIPY photosensitizer for photoacoustic and photothermal imaging guided dual modal cancer phototherapy. Journal of Materials Chemistry B, 2017, 5, 1566-1573.	5.8	96
116	In Situ Synthesis of Reduced Graphene Oxide and Gold Nanocomposites for Nanoelectronics and Biosensing. Nanoscale Research Letters, 2011, 6, 60.	5.7	93
117	High capacitive performance of flexible and binder-free graphene–polypyrrole composite membrane based on in situ reduction of graphene oxide and self-assembly. Nanoscale, 2013, 5, 9860.	5.6	93
118	Digitalized Geometric Phases for Parallel Optical Spin and Orbital Angular Momentum Encoding. ACS Photonics, 2017, 4, 1333-1338.	6.6	93
119	Apelin Attenuates Oxidative Stress in Human Adipocytes. Journal of Biological Chemistry, 2014, 289, 3763-3774.	3.4	92
120	Roles of Cholesterol in Vesicle Fusion and Motion. Biophysical Journal, 2009, 97, 1371-1380.	0.5	91
121	Precisely Aligned Monolayer MoS ₂ Epitaxially Grown on hâ€BN basal Plane. Small, 2017, 13, 1603005.	10.0	91
122	Bifunctional N-CoSe ₂ /3D-MXene as Highly Efficient and Durable Cathode for Rechargeable Zn–Air Battery. , 2019, 1, 432-439.		90
123	Apelin inhibits adipogenesis and lipolysis through distinct molecular pathways. Molecular and Cellular Endocrinology, 2012, 362, 227-241.	3.2	89
124	Insight into the charge transport correlation in Au _x clusters and graphene quantum dots deposited on TiO ₂ nanotubes for photoelectrochemical oxygen evolution. Journal of Materials Chemistry A, 2018, 6, 11154-11162.	10.3	89
125	Electrosynthesis and characterization of polypyrrole/Au nanocomposite. Electrochimica Acta, 2007, 52, 2845-2849.	5.2	88
126	Transdermal Delivery of Antiâ€Obesity Compounds to Subcutaneous Adipose Tissue with Polymeric Microneedle Patches. Small Methods, 2017, 1, 1700269.	8.6	88

#	Article	IF	CITATIONS
127	Carbohydrate functionalized carbon nanotubes and their applications. Chemical Society Reviews, 2010, 39, 2925.	38.1	87
128	Apelin Enhances Brown Adipogenesis and Browning of White Adipocytes. Journal of Biological Chemistry, 2015, 290, 14679-14691.	3.4	87
129	Nanowires assembled from MnCo2O4@C nanoparticles for water splitting and all-solid-state supercapacitor. Nano Research, 2016, 9, 1300-1309.	10.4	87
130	Amperometric Detection of Quantal Catecholamine Secretion from Individual Cells on Micromachined Silicon Chips. Analytical Chemistry, 2003, 75, 518-524.	6.5	86
131	Increase of riboflavin biosynthesis underlies enhancement of extracellular electron transfer of Shewanella in alkaline microbial fuel cells. Bioresource Technology, 2013, 130, 763-768.	9.6	86
132	Meta-q-plate for complex beam shaping. Scientific Reports, 2016, 6, 25528.	3.3	86
133	Simultaneous label-free and pretreatment-free detection of heavy metal ions in complex samples using electrodes decorated with vertically ordered silica nanochannels. Sensors and Actuators B: Chemical, 2018, 259, 364-371.	7.8	86
134	Dualâ€lonâ€Diffusion Induced Degradation in Leadâ€Free Cs ₂ AgBiBr ₆ Double Perovskite Solar Cells. Advanced Functional Materials, 2020, 30, 2002342.	14.9	86
135	Solid-Phase Colorimetric Sensor Based on Gold Nanoparticle-Loaded Polymer Brushes: Lead Detection as a Case Study. Analytical Chemistry, 2013, 85, 4094-4099.	6.5	84
136	The importance of intermediates ring-opening in preventing photocatalyst deactivation during toluene decomposition. Applied Catalysis B: Environmental, 2020, 272, 118977.	20.2	84
137	A highly Ca2+-sensitive pool of vesicles is regulated by protein kinase C in adrenal chromaffin cells. Proceedings of the National Academy of Sciences of the United States of America, 2002, 99, 17060-17065.	7.1	83
138	High-strength carbon nanotube buckypaper composites as applied to free-standing electrodes for supercapacitors. Journal of Materials Chemistry A, 2013, 1, 4057.	10.3	83
139	Strain sensors based on chromium nanoparticle arrays. Nanoscale, 2014, 6, 3930-3933.	5.6	83
140	Ternary Chalcogenide Nanosheets with Ultrahigh Photothermal Conversion Efficiency for Photoacoustic Theranostics. Small, 2017, 13, 1604139.	10.0	83
141	Microwave-assisted solvothermal synthesis of 3D carnation-like SnS2 nanostructures with high visible light photocatalytic activity. Journal of Molecular Catalysis A, 2013, 378, 285-292.	4.8	82
142	Organic Nanoprobe Cocktails for Multilocal and Multicolor Fluorescence Imaging of Reactive Oxygen Species. Advanced Functional Materials, 2017, 27, 1700493.	14.9	82
143	A graphene nanoribbon network and its biosensing application. Nanoscale, 2011, 3, 5156.	5.6	81
144	Theoretical design and experimental investigation on highly selective Pd particles decorated C3N4 for safe photocatalytic NO purification, Journal of Hazardous Materials, 2020, 392, 122357	12.4	81

#	Article	IF	CITATIONS
145	Dynamic transcriptome changes during adipose tissue energy expenditure reveal critical roles for long noncoding RNA regulators. PLoS Biology, 2017, 15, e2002176.	5.6	81
146	Terahertz vortex beam generator based on a photopatterned large birefringence liquid crystal. Optics Express, 2017, 25, 12349.	3.4	79
147	Biâ€based photocatalysts for <scp>lightâ€driven</scp> environmental and energy applications: Structural tuning, reaction mechanisms, and challenges. EcoMat, 2020, 2, e12047.	11.9	79
148	Synergistic photo-thermal catalytic NO purification of MnO /g-C3N4: Enhanced performance and reaction mechanism. Chinese Journal of Catalysis, 2018, 39, 619-629.	14.0	75
149	Graphene wrapped SnCo nanoparticles for high-capacity lithium ion storage. Journal of Power Sources, 2013, 222, 526-532.	7.8	73
150	The Electrical Detection of Lead Ions Using Goldâ€Nanoparticle―and DNAzymeâ€Functionalized Graphene Device. Advanced Healthcare Materials, 2013, 2, 271-274.	7.6	73
151	Intermarriage of Halide Perovskites and Metalâ€Organic Framework Crystals. Angewandte Chemie - International Edition, 2020, 59, 19434-19449.	13.8	73
152	Micro- and Nanotechnologies for Study of Cell Secretion. Analytical Chemistry, 2011, 83, 4393-4406.	6.5	72
153	Monitoring Dynamic Cellular Redox Homeostasis Using Fluorescence-Switchable Graphene Quantum Dots. ACS Nano, 2016, 10, 11475-11482.	14.6	71
154	Gold nanoparticles decorated reduced graphene oxide for detecting the presence and cellular release of nitric oxide. Electrochimica Acta, 2013, 111, 441-446.	5.2	69
155	Liquid crystal integrated metalens with tunable chromatic aberration. Advanced Photonics, 2020, 2, 1.	11.8	68
156	Tunable Electroluminescence in Planar Graphene/SiO ₂ Memristors. Advanced Materials, 2013, 25, 5593-5598.	21.0	67
157	Multi-stimuli responsive smart chitosan-based microcapsules for targeted drug delivery and triggered drug release. Ultrasonics Sonochemistry, 2017, 38, 145-153.	8.2	67
158	Pivotal roles of artificial oxygen vacancies in enhancing photocatalytic activity and selectivity on Bi2O2CO3 nanosheets. Chinese Journal of Catalysis, 2019, 40, 620-630.	14.0	65
159	Ultrafast growth of large single crystals of monolayer WS2 and WSe2. National Science Review, 2020, 7, 737-744.	9.5	64
160	Direct van der Waals epitaxial growth of 1D/2D Sb2Se3/WS2 mixed-dimensional p-n heterojunctions. Nano Research, 2019, 12, 1139-1145.	10.4	63
161	Label-free detection of ATP release from living astrocytes with high temporal resolution using carbon nanotube network. Biosensors and Bioelectronics, 2009, 24, 2716-2720.	10.1	62
162	Design of twin junction with solid solution interface for efficient photocatalytic H2 production. Nano Energy, 2020, 69, 104410.	16.0	62

#	Article	IF	CITATIONS
163	Gate tunable MoS ₂ –black phosphorus heterojunction devices. 2D Materials, 2015, 2, 034009.	4.4	61
164	Light-Induced Generation and Regeneration of Oxygen Vacancies in BiSbO ₄ for Sustainable Visible Light Photocatalysis. ACS Applied Materials & Interfaces, 2019, 11, 47984-47991.	8.0	61
165	Programmable devices based on reversible solid-state doping of two-dimensional semiconductors with superionic silver iodide. Nature Electronics, 2020, 3, 630-637.	26.0	61
166	Rolling Up a Monolayer MoS ₂ Sheet. Small, 2016, 12, 3770-3774.	10.0	60
167	Gate tunable WSe ₂ –BP van der Waals heterojunction devices. Nanoscale, 2016, 8, 3254-3258.	5.6	60
168	Cobalt Phosphide Double-Shelled Nanocages: Broadband Light-Harvesting Nanostructures for Efficient Photothermal Therapy and Self-Powered Photoelectrochemical Biosensing. Small, 2017, 13, 1700798.	10.0	60
169	Quasi-homogeneous carbocatalysis for one-pot selective conversion of carbohydrates to 5-hydroxymethylfurfural using sulfonated graphene quantum dots. Carbon, 2018, 136, 224-233.	10.3	60
170	Growth of Single-Crystalline Cadmium Iodide Nanoplates, CdI ₂ /MoS ₂ (WS ₂ , WSe ₂) van der Waals Heterostructures, and Patterned Arrays. ACS Nano, 2017, 11, 3413-3419.	14.6	59
171	Synthesis of 2D Layered Bil ₃ Nanoplates, Bil ₃ /WSe ₂ van der Waals Heterostructures and Their Electronic, Optoelectronic Properties. Small, 2017, 13, 1701034.	10.0	59
172	Broadband Detection of Multiple Spin and Orbital Angular Momenta via Dielectric Metasurface. Laser and Photonics Reviews, 2020, 14, 2000062.	8.7	58
173	Control of Adipogenesis by the Autocrine Interplays between Angiotensin 1–7/Mas Receptor and Angiotensin II/AT1 Receptor Signaling Pathways. Journal of Biological Chemistry, 2013, 288, 15520-15531.	3.4	57
174	Microfiber devices based on carbon materials. Materials Today, 2015, 18, 215-226.	14.2	57
175	Unveiling the unconventional roles of methyl number on the ring-opening barrier in photocatalytic decomposition of benzene, toluene and o-xylene. Applied Catalysis B: Environmental, 2020, 278, 119318.	20.2	57
176	Approaching the intrinsic exciton physics limit in two-dimensional semiconductor diodes. Nature, 2021, 599, 404-410.	27.8	57
177	Polarization-controllable Airy beams generated via a photoaligned director-variant liquid crystal mask. Scientific Reports, 2015, 5, 17484.	3.3	55
178	Generation of Equal-Energy Orbital Angular Momentum Beams via Photopatterned Liquid Crystals. Physical Review Applied, 2016, 5, .	3.8	55
179	Ultra-sensitive detection of adipocytokines with CMOS-compatible silicon nanowire arrays. Nanoscale, 2009, 1, 159.	5.6	54
180	Changes in Brain Cholesterol Metabolome After Excitotoxicity. Molecular Neurobiology, 2010, 41, 299-313.	4.0	54

#	Article	IF	CITATIONS
181	Liquid-crystal-integrated metadevice: towards active multifunctional terahertz wave manipulations. Optics Letters, 2018, 43, 4695.	3.3	54
182	Alkaline-earth bis(trifluoromethanesulfonimide) additives for efficient and stable perovskite solar cells. Nano Energy, 2020, 69, 104412.	16.0	54
183	Comparative transcriptomic analysis reveals key genes and pathways in two different cadmium tolerance kenaf (Hibiscus cannabinus L.) cultivars. Chemosphere, 2021, 263, 128211.	8.2	53
184	Nanoelectronic detection of triggered secretion of pro-inflammatory cytokines using CMOS compatible silicon nanowires. Biosensors and Bioelectronics, 2011, 26, 2746-2750.	10.1	52
185	Chemical Vapor Deposition Growth of Single Crystalline CoTe ₂ Nanosheets with Tunable Thickness and Electronic Properties. Chemistry of Materials, 2018, 30, 8891-8896.	6.7	51
186	Small-molecule diketopyrrolopyrrole-based therapeutic nanoparticles for photoacoustic imaging-guided photothermal therapy. Nano Research, 2017, 10, 794-801.	10.4	50
187	Holey nickel hydroxide nanosheets for wearable solid-state fiber-supercapacitors. Nanoscale, 2018, 10, 5442-5448.	5.6	50
188	Facet-dependent photocatalytic NO conversion pathways predetermined by adsorption activation patterns. Nanoscale, 2019, 11, 2366-2373.	5.6	49
189	A Portable and Efficient Solarâ€Rechargeable Battery with Ultrafast Photoâ€Charge/Discharge Rate. Advanced Energy Materials, 2019, 9, 1900872.	19.5	49
190	Sugarâ€Based Synthesis of Tamiflu and Its Inhibitory Effects on Cell Secretion. Chemistry - A European Journal, 2010, 16, 4533-4540.	3.3	48
191	The high selectivity for benzoic acid formation on Ca2Sb2O7 enables efficient and stable toluene mineralization. Applied Catalysis B: Environmental, 2020, 271, 118948.	20.2	48
192	Weavable, Highâ€Performance, Solid‣tate Supercapacitors Based on Hybrid Fibers Made of Sandwiched Structure of MWCNT/rGO/MWCNT. Advanced Electronic Materials, 2016, 2, 1600102.	5.1	47
193	Molecular‣evel Design of Hierarchically Porous Carbons Codoped with Nitrogen and Phosphorus Capable of In Situ Selfâ€Activation for Sustainable Energy Systems. Small, 2017, 13, 1602010.	10.0	47
194	Vortex Airy beams directly generated via liquid crystal q-Airy-plates. Applied Physics Letters, 2018, 112, .	3.3	47
195	Luminescent europium-doped titania for efficiency and UV-stability enhancement of planar perovskite solar cells. Nano Energy, 2020, 69, 104392.	16.0	47
196	Integrating carbon nanotubes and lipid bilayer for biosensing. Biosensors and Bioelectronics, 2010, 25, 1834-1837.	10.1	46
197	A General Route Towards Defect and Pore Engineering in Graphene. Small, 2014, 10, 2280-2284.	10.0	46
198	The electrical properties of graphene modified by bromophenyl groups derived from a diazonium compound. Carbon, 2012, 50, 1517-1522.	10.3	45

#	Article	IF	CITATIONS
199	Transcriptome analysis revealed key genes and pathways related to cadmium-stress tolerance in Kenaf (Hibiscus cannabinus L.). Industrial Crops and Products, 2020, 158, 112970.	5.2	45
200	Vortex-controlled morphology conversion of microstructures on silicon induced by femtosecond vector vortex beams. Applied Physics Letters, 2017, 111, .	3.3	44
201	Complete sequence of kenaf (Hibiscus cannabinus) mitochondrial genome and comparative analysis with the mitochondrial genomes of other plants. Scientific Reports, 2018, 8, 12714.	3.3	43
202	Minimizing Voltage Losses in Perovskite Solar Cells. Small Structures, 2021, 2, 2000050.	12.0	43
203	Graphene quantum dots assisted exfoliation of atomically-thin 2D materials and as-formed 0D/2D van der Waals heterojunction for HER. Carbon, 2021, 184, 554-561.	10.3	43
204	Nanoelectronic Biosensing of Dynamic Cellular Activities Based on Nanostructured Materials. Advanced Materials, 2010, 22, 2818-2823.	21.0	42
205	Enzymeless multi-sugar fuel cells with high power output based on 3D graphene–Co3O4 hybrid electrodes. Physical Chemistry Chemical Physics, 2013, 15, 9170.	2.8	42
206	Beam shaping via photopatterned liquid crystals. Liquid Crystals, 2016, 43, 2051-2061.	2.2	42
207	Smectic Layer Origami via Preprogrammed Photoalignment. Advanced Materials, 2017, 29, 1606671.	21.0	42
208	Graphene quantum dots based fluorescence turn-on nanoprobe for highly sensitive and selective imaging of hydrogen sulfide in living cells. Biomaterials Science, 2018, 6, 779-784.	5.4	42
209	Jâ€Aggregateâ€Based FRET Monitoring of Drug Release from Polymer Nanoparticles with High Drug Loading. Angewandte Chemie - International Edition, 2020, 59, 20065-20074.	13.8	42
210	Facet-Dependent Catalytic Performance of Au Nanocrystals for Electrochemical Nitrogen Reduction. ACS Applied Materials & Interfaces, 2020, 12, 41613-41619.	8.0	42
211	Modulating PL and electronic structures of MoS2/graphene heterostructures via interlayer twisting angle. Applied Physics Letters, 2017, 111, .	3.3	41
212	Sonochemical fabrication of folic acid functionalized multistimuli-responsive magnetic graphene oxide-based nanocapsules for targeted drug delivery. Chemical Engineering Journal, 2017, 326, 839-848.	12.7	40
213	Remodeling Tumor Microenvironment by Multifunctional Nanoassemblies for Enhanced Photodynamic Cancer Therapy. , 2020, 2, 1268-1286.		40
214	Redox Control of Charge Transport in Vertical Ferrocene Molecular Tunnel Junctions. CheM, 2020, 6, 1172-1182.	11.7	40
215	Diketopyrrolopyrrole-Based Photosensitizers Conjugated with Chemotherapeutic Agents for Multimodal Tumor Therapy. ACS Applied Materials & Interfaces, 2017, 9, 30398-30405.	8.0	39
216	Self-Assembled Asymmetric Microlenses for Four-Dimensional Visual Imaging. ACS Nano, 2019, 13, 13709-13715.	14.6	39

#	Article	IF	CITATIONS
217	Vesicular storage, vesicle trafficking, and secretion of leptin and resistin: the similarities, differences, and interplays. Journal of Endocrinology, 2010, 206, 27-36.	2.6	38
218	Fast-response and high-efficiency optical switch based on dual-frequency liquid crystal polarization grating. Optical Materials Express, 2016, 6, 597.	3.0	38
219	Phenethylammonium bismuth halides: from single crystals to bulky-organic cation promoted thin-film deposition for potential optoelectronic applications. Journal of Materials Chemistry A, 2019, 7, 20733-20741.	10.3	38
220	Label-Free Electronic Detection of DNA Using Simple Double-Walled Carbon Nanotube Resistors. Journal of Physical Chemistry C, 2008, 112, 9891-9895.	3.1	37
221	Graphene oxide mediated co-generation of C-doping and oxygen defects in Bi ₂ WO ₆ nanosheets: a combined DRIFTS and DFT investigation. Nanoscale, 2019, 11, 20562-20570.	5.6	37
222	A Route toward Digital Manipulation of Water Nanodroplets on Surfaces. ACS Nano, 2014, 8, 3955-3960.	14.6	35
223	Ultra-sensitive and wide-dynamic-range sensors based on dense arrays of carbon nanotube tips. Nanoscale, 2011, 3, 4854.	5.6	34
224	Synthesis of ultrathin two-dimensional nanosheets and van der Waals heterostructures from non-layered γ-Cul. Npj 2D Materials and Applications, 2018, 2, .	7.9	34
225	Promoted reactants activation and charge separation leading to efficient photocatalytic activity on phosphate/potassium co-functionalized carbon nitride. Chinese Chemical Letters, 2019, 30, 875-880.	9.0	34
226	Solution-processable semiconducting thin-film transistors using single-walled carbon nanotubes chemically modified by organic radical initiators. Chemical Communications, 2009, , 7182.	4.1	33
227	Gallium-Doped Tin Oxide Nano-Cuboids for Improved Dye Sensitized Solar Cell. ACS Applied Materials & Interfaces, 2013, 5, 11377-11382.	8.0	33
228	Transcriptome de novo assembly and differentially expressed genes related to cytoplasmic male sterility in kenaf (Hibiscus cannabinus L.). Molecular Breeding, 2014, 34, 1879-1891.	2.1	33
229	Graphene quantum dots for ultrasensitive detection of acetylcholinesterase and its inhibitors. 2D Materials, 2015, 2, 034018.	4.4	33
230	Lead-free metal-halide double perovskites: from optoelectronic properties to applications. Nanophotonics, 2021, 10, 2181-2219.	6.0	33
231	Effects of cholesterol oxidation products on exocytosis. Neuroscience Letters, 2010, 476, 36-41.	2.1	32
232	Broadband Plasmonic Antenna Enhanced Upconversion and Its Application in Flexible Fingerprint Identification. Advanced Optical Materials, 2018, 6, 1701119.	7.3	32
233	Semiconducting Polymer Nanobiocatalysts for Photoactivation of Intracellular Redox Reactions. Angewandte Chemie - International Edition, 2018, 57, 13484-13488.	13.8	32
234	High-performance asymmetric electrodes photodiode based on Sb/WSe2 heterostructure. Nano Research, 2019, 12, 339-344.	10.4	32

#	Article	IF	CITATIONS
235	Transdermal Photothermal-Pharmacotherapy to Remodel Adipose Tissue for Obesity and Metabolic Disorders. ACS Nano, 2022, 16, 1813-1825.	14.6	32
236	Fluorescence quenching between unbonded graphene quantum dots and gold nanoparticles upon simple mixing. RSC Advances, 2014, 4, 35673-35677.	3.6	31
237	Perfect Higher-Order Poincaré Sphere Beams from Digitalized Geometric Phases. Physical Review Applied, 2018, 10, .	3.8	31
238	Planar Terahertz Photonics Mediated by Liquid Crystal Polymers. Advanced Optical Materials, 2020, 8, 1902124.	7.3	31
239	Electrodeposition of hierarchical MnO2 spheres for enzyme immobilization and glucose biosensing. Journal of Materials Chemistry B, 2013, 1, 2696.	5.8	30
240	Fluorescent quantum dots derived from PEDOT and their applications in optical imaging and sensing. Materials Horizons, 2014, 1, 529-534.	12.2	30
241	Four‣ayer Tin–Carbon Nanotube Yolk–Shell Materials for Highâ€Performance Lithiumâ€ŀon Batteries. ChemSusChem, 2014, 7, 1407-1414.	6.8	30
242	Graphene–bacteria composite for oxygen reduction and lithium ion batteries. Journal of Materials Chemistry A, 2015, 3, 12873-12879.	10.3	30
243	Optical array generator based on blue phase liquid crystal Dammann grating. Optical Materials Express, 2016, 6, 1087.	3.0	30
244	RNA Binding Protein Ybx2 Regulates RNA Stability During Cold-Induced Brown Fat Activation. Diabetes, 2017, 66, 2987-3000.	0.6	30
245	Two-dimensional plumbum-doped tin diselenide monolayer transistor with high on/off ratio. Nanotechnology, 2018, 29, 474002.	2.6	30
246	Lightâ€Activated Liquid Crystalline Hierarchical Architecture Toward Photonics. Advanced Optical Materials, 2019, 7, 1900393.	7.3	29
247	Dimensionality-Controlled Surface Passivation for Enhancing Performance and Stability of Perovskite Solar Cells via Triethylenetetramine Vapor. ACS Applied Materials & Interfaces, 2020, 12, 6651-6661.	8.0	29
248	Multifunctional Liquid Crystal Device for Grayscale Pattern Display and Holography with Tunable Spectralâ€Response. Laser and Photonics Reviews, 2022, 16, .	8.7	29
249	Template-free synthesis of large anisotropic gold nanostructures on reduced graphene oxide. Nanoscale, 2012, 4, 3055.	5.6	28
250	Regulatory networks of non-coding RNAs in brown/beige adipogenesis. Bioscience Reports, 2015, 35, .	2.4	28
251	Magnetotransport Properties of Graphene Nanoribbons with Zigzag Edges. Physical Review Letters, 2018, 120, 216601.	7.8	28
252	Antimicrobial Microneedle Patch for Treating Deep Cutaneous Fungal Infection. Advanced Therapeutics, 2019, 2, 1900064.	3.2	28

#	Article	IF	CITATIONS
253	Sulfur-based redox chemistry for electrochemical energy storage. Coordination Chemistry Reviews, 2020, 422, 213445.	18.8	28
254	2D single- or double-layered vanadium oxide nanosheet assembled 3D microflowers: controlled synthesis, growth mechanism, and applications. Nanoscale, 2013, 5, 7790.	5.6	27
255	5-azacytidine pre-treatment alters DNA methylation levels and induces genes responsive to salt stress in kenaf (Hibiscus cannabinus L.). Chemosphere, 2021, 271, 129562.	8.2	27
256	Nonâ€invasive Detection of Cellular Bioelectricity Based on Carbon Nanotube Devices for Highâ€Throughput Drug Screening. Advanced Materials, 2010, 22, 3199-3203.	21.0	26
257	Fabrication and characterization of recyclable carbon nanotube/polyvinyl butyral composite fiber. Composites Science and Technology, 2011, 71, 1665-1670.	7.8	26
258	Liquid crystal depolarizer based on photoalignment technology. Photonics Research, 2016, 4, 70.	7.0	26
259	Recent advances in lowâ€ŧoxic leadâ€free metal halide perovskite materials for solar cell application. Asia-Pacific Journal of Chemical Engineering, 2016, 11, 392-398.	1.5	26
260	Inorganic pâ€Type Semiconductors as Hole Conductor Building Blocks for Robust Perovskite Solar Cells. Advanced Sustainable Systems, 2018, 2, 1800032.	5.3	26
261	Tunable band-pass optical vortex processor enabled by wash-out-refill chiral superstructures. Applied Physics Letters, 2021, 118, .	3.3	26
262	Differential effects of ceramide species on exocytosis in rat PC12 cells. Experimental Brain Research, 2007, 183, 241-247.	1.5	25
263	Substrate Engineering for CVD Growth of Single Crystal Graphene. Small Methods, 2021, 5, e2001213.	8.6	25
264	Nanoconfined Topochemical Conversion from MXene to Ultrathin Non‣ayered TiN Nanomesh toward Superior Electrocatalysts for Lithiumâ€Sulfur Batteries. Small, 2021, 17, e2101360.	10.0	25
265	Nanotopographic Carbon Nanotube Thinâ€Film Substrate Freezes Lateral Motion of Secretory Vesicles. Advanced Materials, 2009, 21, 790-793.	21.0	24
266	Iron Oxide Nanoparticle-Powered Micro-Optical Coherence Tomography for in Situ Imaging the Penetration and Swelling of Polymeric Microneedles in the Skin. ACS Applied Materials & Interfaces, 2017, 9, 20340-20347.	8.0	24
267	Achievement of significantly improved lithium storage for novel clew-like Li 4 Ti 5 O 12 anode assembled by ultrafine nanowires. Journal of Power Sources, 2017, 350, 49-55.	7.8	24
268	Enhanced plasmonic photocatalytic disinfection on noble-metal-free bismuth nanospheres/graphene nanocomposites. Catalysis Science and Technology, 2018, 8, 4600-4603.	4.1	24
269	Molecular cloning and subcellular localization of six HDACs and their roles in response to salt and drought stress in kenaf (Hibiscus cannabinus L.). Biological Research, 2019, 52, 20.	3.4	24
270	Liquid crystal devices for vector vortex beams manipulation and quantum information applications [Invited]. Chinese Optics Letters, 2021, 19, 112601.	2.9	24

#	Article	IF	CITATIONS
271	Detecting metabolic activities of bacteria using a simple carbon nanotube device for high-throughput screening of anti-bacterial drugs. Biosensors and Bioelectronics, 2011, 26, 4257-4261.	10.1	23
272	Generation of self-healing and transverse accelerating optical vortices. Applied Physics Letters, 2016, 109, .	3.3	23
273	Comparative phosphoproteomic analysis reveals differentially phosphorylated proteins regulate anther and pollen development in kenaf cytoplasmic male sterility line. Amino Acids, 2018, 50, 841-862.	2.7	23
274	Flexible solar-rechargeable energy system. Energy Storage Materials, 2020, 32, 356-376.	18.0	23
275	Nanopore Unstacking of Single-Stranded DNA Helices. Small, 2007, 3, 1204-1208.	10.0	22
276	An Interwoven Network of MnO ₂ Nanowires and Carbon Nanotubes as the Anode for Bendable Lithiumâ€lon Batteries. ChemPhysChem, 2014, 15, 2445-2449.	2.1	22
277	Solution-processed flexible transparent conductors based on carbon nanotubes and silver grid hybrid films. Nanoscale, 2014, 6, 4560-4565.	5.6	22
278	TiN@VN Nanowire Arrays on 3D Carbon for Highâ€Performance Supercapacitors. ChemElectroChem, 2014, 1, 1027-1030.	3.4	22
279	An elaborate strategy for fabricating one-dimensional quasi-hollow nanostructure of tin dioxide@carbon composite with improved lithium storage performance. Carbon, 2017, 118, 634-641.	10.3	22
280	Enhancing electrochemical nitrogen reduction with Ru nanowires <i>via</i> the atomic decoration of Pt. Journal of Materials Chemistry A, 2020, 8, 25142-25147.	10.3	22
281	Examining second-harmonic generation of high-order Laguerre–Gaussian modes through a single cylindrical lens. Optics Letters, 2017, 42, 4387.	3.3	22
282	Involvement of PKCα in PMA-induced facilitation of exocytosis and vesicle fusion in PC12 cells. Biochemical and Biophysical Research Communications, 2009, 380, 371-376.	2.1	21
283	The crosstalks between adipokines and catecholamines. Molecular and Cellular Endocrinology, 2011, 332, 261-270.	3.2	21
284	Apelin secretion and expression of apelin receptors in 3T3-L1 adipocytes are differentially regulated by angiotensin type 1 and type 2 receptors. Molecular and Cellular Endocrinology, 2012, 351, 296-305.	3.2	21
285	Nanoporous tin oxide photoelectrode prepared by electrochemical anodization in aqueous ammonia to improve performance of dye sensitized solar cell. Journal of Renewable and Sustainable Energy, 2013, 5, 023120.	2.0	21
286	Colorimetric surface plasmon resonance imaging (SPRI) biosensor array based on polarization orientation. Biosensors and Bioelectronics, 2013, 47, 545-552.	10.1	21
287	Graphene nanoribbons epitaxy on boron nitride. Applied Physics Letters, 2016, 108, .	3.3	21
288	A Graphene Quantum Dots–Hypochlorite Hybrid System for the Quantitative Fluorescent Determination of Total Antioxidant Capacity. Small, 2017, 13, 1700709.	10.0	21

#	Article	IF	CITATIONS
289	Programmable self-propelling actuators enabled by a dynamic helical medium. Science Advances, 2021, 7, .	10.3	21
290	Carbon-based spintronics. Science China: Physics, Mechanics and Astronomy, 2013, 56, 207-221.	5.1	20
291	Fabrication of high-quality all-graphene devices with low contact resistances. Nano Research, 2014, 7, 1449-1456.	10.4	20
292	Patterning monolayer graphene with zigzag edges on hexagonal boron nitride by anisotropic etching. Applied Physics Letters, 2016, 109, .	3.3	20
293	Helicity-dependent forked vortex lens based on photo-patterned liquid crystals. Optics Express, 2017, 25, 14059.	3.4	20
294	Tunable excitonic emission of monolayer WS2 for the optical detection of DNA nucleobases. Nano Research, 2018, 11, 1744-1754.	10.4	20
295	Controlling the secondary pollutant on B-doped g-C ₃ N ₄ during photocatalytic NO removal: a combined DRIFTS and DFT investigation. Catalysis Science and Technology, 2019, 9, 4531-4537.	4.1	20
296	Comparative Cytological and Gene Expression Analysis Reveals Potential Metabolic Pathways and Target Genes Responsive to Salt Stress in Kenaf (Hibiscus cannabinus L.). Journal of Plant Growth Regulation, 2020, 39, 1245-1260.	5.1	20
297	Highly Selective Synthesis of Monolayer or Bilayer WSe ₂ Single Crystals by Pre-annealing the Solid Precursor. Chemistry of Materials, 2021, 33, 1307-1313.	6.7	20
298	Differential effects of lysophospholipids on exocytosis in rat PC12 cells. Journal of Neural Transmission, 2010, 117, 301-308.	2.8	19
299	Macroporous foam of reduced graphene oxides prepared by lyophilization. Materials Research Bulletin, 2012, 47, 4335-4339.	5.2	18
300	The Effect of Twin Grain Boundary Tuned by Temperature on the Electrical Transport Properties of Monolayer MoS2. Crystals, 2016, 6, 115.	2.2	18
301	Fragmentation of twisted light in photon–phonon nonlinear propagation. Applied Physics Letters, 2018, 112, .	3.3	18
302	Effects of phorbol ester on vesicle dynamics as revealed by total internal reflection fluorescence microscopy. Pflugers Archiv European Journal of Physiology, 2008, 457, 211-222.	2.8	17
303	Assessment of (n,m) Selectively Enriched Small Diameter Single-Walled Carbon Nanotubes by Density Differentiation from Cobalt-Incorporated MCM-41 for Macroelectronics. Chemistry of Materials, 2008, 20, 7417-7424.	6.7	17
304	Anticancer Efficacy and Subcellular Site of Action Investigated by Realâ€Time Monitoring of Cellular Responses to Localized Drug Delivery in Single Cells. Small, 2012, 8, 2670-2674.	10.0	17
305	Transdermal theranostics. View, 2020, 1, e21.	5.3	17
306	Ultrafast switching of optical singularity eigenstates with compact integrable liquid crystal structures. Optics Express, 2018, 26, 28818.	3.4	17

#	Article	IF	CITATIONS
307	Fullâ€Stokes Polarimetry for Visible Light Enabled by an Allâ€Dielectric Metasurface. Advanced Photonics Research, 2022, 3, .	3.6	17
308	Generation of strong cylindrical vector pulses via stimulated Brillouin amplification. Applied Physics Letters, 2017, 110, .	3.3	16
309	Generating, Separating and Polarizing Terahertz Vortex Beams via Liquid Crystals with Gradient-Rotation Directors. Crystals, 2017, 7, 314.	2.2	16
310	Bidirectional mediation of TiO2 nanowires field effect transistor by dipole moment from purple membrane. Nanoscale, 2010, 2, 1474.	5.6	15
311	Mobility Enhancement in Carbon Nanotube Transistors by Screening Charge Impurity with Silica Nanoparticles. Journal of Physical Chemistry C, 2011, 115, 6975-6979.	3.1	15
312	Integrated and reconfigurable optical paths based on stacking optical functional films. Optics Express, 2016, 24, 25510.	3.4	15
313	Analysis of chloroplast differences in leaves of rice isonuclear alloplasmic lines. Protoplasma, 2018, 255, 863-871.	2.1	15
314	Control the orbital angular momentum in third-harmonic generation using quasi-phase-matching. Optics Express, 2018, 26, 17563.	3.4	15
315	Energy loss analysis in photoelectrochemical water splitting: a case study of hematite photoanodes. Physical Chemistry Chemical Physics, 2018, 20, 22629-22635.	2.8	15
316	A Fast-Response and Helicity-Dependent Lens Enabled by Micro-Patterned Dual-Frequency Liquid Crystals. Crystals, 2019, 9, 111.	2.2	15
317	Switchable Secondâ€Harmonic Generation of Airy Beam and Airy Vortex Beam. Advanced Optical Materials, 2021, 9, 2001776.	7.3	15
318	Physiological and DNA methylation analysis provides epigenetic insights into chromium tolerance in kenaf. Environmental and Experimental Botany, 2022, 194, 104684.	4.2	15
319	Analogous Optical Activity in Free Space Using a Single Pancharatnam–Berry Phase Element. Laser and Photonics Reviews, 2022, 16, 2100291.	8.7	15
320	Fabrication of transparent and conductive carbon nanotube/polyvinyl butyral films by a facile solution surface dip coating method. Nanoscale, 2011, 3, 2469.	5.6	14
321	Nacre Mimetic with Embedded Silver Nanowire for Resistive Heating. ACS Applied Nano Materials, 2018, 1, 940-952.	5.0	14
322	Intermarriage of Halide Perovskites and Metalâ€Organic Framework Crystals. Angewandte Chemie, 2020, 132, 19602-19617.	2.0	14
323	Smectic Defect Engineering Enabled by Programmable Photoalignment. Advanced Optical Materials, 2020, 8, 2000593.	7.3	14
324	Designing efficient Bi ₂ Fe ₄ O ₉ photoanodes <i>via</i> bulk and surface defect engineering. Chemical Communications, 2020, 56, 9376-9379.	4.1	14

#	Article	IF	CITATIONS
325	Spectral and spatial characterization of upconversion luminescent nanocrystals as nanowaveguides. Nanoscale, 2017, 9, 9238-9245.	5.6	13
326	Multiple generations of high-order orbital angular momentum modes through cascaded third-harmonic generation in a 2D nonlinear photonic crystal. Optics Express, 2017, 25, 11556.	3.4	13
327	Surface immobilized cholera toxin B subunit (CTB) facilitates vesicle docking, trafficking and exocytosis. Integrative Biology (United Kingdom), 2010, 2, 250.	1.3	12
328	Liquidâ€Crystalâ€Mediated Active Waveguides toward Programmable Integrated Optics. Advanced Optical Materials, 2020, 8, 1902033.	7.3	12
329	Dynamically Selective and Simultaneous Detection of Spin and Orbital Angular Momenta of Light with Thermoresponsive Self-Assembled Chiral Superstructures. ACS Photonics, 2022, 9, 1050-1057.	6.6	12
330	Labeling and Tracking P2 Purinergic Receptors in Living Cells Using ATPâ€Conjugated Quantum Dots. Advanced Functional Materials, 2011, 21, 2776-2780.	14.9	11
331	A comparative study of the atp9 gene between a cytoplasmic male sterile line and its maintainer line and further development of a molecular marker specific for male sterile cytoplasm in kenaf (Hibiscus) Tj ETQq1	1 0. 7.8 431	4 rg&T /Over
332	Thiophene-derived polymer dots for imaging endocytic compartments in live cells and broad-spectrum bacterial killing. Materials Chemistry Frontiers, 2017, 1, 152-157.	5.9	11
333	Spin-controlled massive channels of hybrid-order Poincaré sphere beams. Applied Physics Letters, 2020, 117, .	3.3	11
334	iTRAQ-based comparative proteomic response analysis reveals regulatory pathways and divergent protein targets associated with salt-stress tolerance in kenaf (Hibiscus cannabinus L.). Industrial Crops and Products, 2020, 153, 112566.	5.2	11
335	Visible and Online Detection of Nearâ€Infrared Optical Vortices via Nonlinear Photonic Crystals. Advanced Optical Materials, 2022, 10, 2101098.	7.3	11
336	PKC epsilon facilitates recovery of exocytosis after an exhausting stimulation. Pflugers Archiv European Journal of Physiology, 2009, 458, 1137-1149.	2.8	10
337	Aromatic Molecules Doping in Single-Layer Graphene Probed by Raman Spectroscopy and Electrostatic Force Microscopy. Japanese Journal of Applied Physics, 2010, 49, 01AH04.	1.5	10
338	Tuning Enhancement Efficiency of Multiple Emissive Centers in Graphene Quantum Dots by Core–Shell Plasmonic Nanoparticles. Journal of Physical Chemistry Letters, 2017, 8, 5673-5679.	4.6	10
339	Integrative analyses of translatome and transcriptome reveal important translational controls in brown and white adipose regulated by microRNAs. Scientific Reports, 2017, 7, 5681.	3.3	10
340	Ferroelectric liquid crystal mediated fast switchable orbital angular momentum of light. Optics Express, 2019, 27, 36903.	3.4	10
341	Effects of substrates on photocurrents from photosensitive polymer coated carbon nanotube networks. Applied Physics Letters, 2008, 92, .	3.3	9
342	Kainate Receptors Mediate Regulated Exocytosis of Secretory Phospholipase A2 in SH-SY5Y Neuroblastoma Cells. NeuroSignals, 2012, 20, 72-85.	0.9	9

#	Article	IF	CITATIONS
343	In Situ Charge-Transfer-Induced Transition from Metallic to Semiconducting Single-Walled Carbon Nanotubes. Chemistry of Materials, 2013, 25, 4464-4470.	6.7	9
344	Band evolution of two-dimensional transition metal dichalcogenides under electric fields. Applied Physics Letters, 2019, 115, 083104.	3.3	9
345	Understanding the roles of carbon in carbon/g-C3N4 based photocatalysts for H2 evolution. Nano Research, 0, , 1.	10.4	9
346	Controlling armchair and zigzag edges in oxidative cutting of graphene. Journal of Materials Chemistry C, 2016, 4, 6539-6545.	5.5	8
347	Comparative acetylomic analysis reveals differentially acetylated proteins regulating anther and pollen development in kenaf cytoplasmic male sterility line. Physiologia Plantarum, 2019, 166, 960-978.	5.2	8
348	Lancing Drug Reservoirs into Subcutaneous Fat to Combat Obesity and Associated Metabolic Diseases. Small, 2020, 16, 2002872.	10.0	8
349	Dynamic quantitative photothermal monitoring of cell death of individual human red blood cells upon glucose depletion. Journal of Biomedical Optics, 2010, 15, 057001.	2.6	7
350	Tailoring the photon spin via light–matter interaction in liquid-crystal-based twisting structures. Npj Quantum Materials, 2017, 2, .	5.2	7
351	High-order minibands and interband Landau level reconstruction in graphene moiré superlattices. Physical Review B, 2020, 102, .	3.2	7
352	The transcription factor HcERF4 confers salt and drought tolerance in kenaf (Hibiscus cannabinus L.). Plant Cell, Tissue and Organ Culture, 2022, 150, 207-221.	2.3	7
353	Optical field control via liquid crystal photoalignment. Molecular Crystals and Liquid Crystals, 2017, 644, 3-11.	0.9	6
354	Bulk SnO @C composite for improved lithium storage. Journal of Alloys and Compounds, 2018, 740, 312-320.	5.5	6
355	Evolution of orbital angular momentum in a soft quasi-periodic structure with topological defects. Optics Express, 2019, 27, 21667.	3.4	6
356	On-chip diameter-dependent conversion of metallic to semiconducting single-walled carbon nanotubes by immersion in 2-ethylanthraquinone. RSC Advances, 2012, 2, 1275-1281.	3.6	5
357	Identification of a novel cytoplasmic male sterile line M2BS induced by partial-length HcPDIL5-2a transformation in rice (Oryza sativa L.). Journal of Plant Biology, 2017, 60, 146-153.	2.1	5
358	Comparative profile analysis reveals differentially expressed microRNAs regulate anther and pollen development in kenaf cytoplasmic male sterility line. Genome, 2019, 62, 455-466.	2.0	5
359	A comprehensive integrated transcriptome and metabolome analyses to reveal key genes and essential metabolic pathways involved in CMS in kenaf. Plant Cell Reports, 2021, 40, 223-236.	5.6	5
360	Integrated Methylome and Transcriptome Analyses Reveal the Molecular Mechanism by Which DNA Methylation Regulates Kenaf Flowering. Frontiers in Plant Science, 2021, 12, 709030.	3.6	5

#	Article	IF	CITATIONS
361	Simultaneous Fabrication of Very High Aspect Ratio Positive Nano- to Milliscale Structures. Small, 2009, 5, 1043-1050.	10.0	4
362	Cloning and characterization of novel low molecular weight glutenin subunit genes from two Aegilops species with the C and D genomes. Genetic Resources and Crop Evolution, 2010, 57, 881-890.	1.6	4
363	Fabrication and Characterization of Networked Graphene Devices Based on Ultralarge Single-Layer Graphene Sheets. IEEE Nanotechnology Magazine, 2011, 10, 467-471.	2.0	4
364	Defect-enhanced coupling between graphene and SiO2 substrate. Applied Physics Letters, 2014, 105, 063113.	3.3	4
365	Comparative Proteomics Study on Anther Mitochondria between Cytoplasmic Male Sterility Line and its Maintainer in Kenaf (Hibiscus cannabinus L.). Crop Science, 2014, 54, 1103-1114.	1.8	3
366	A Novel Electroactive Polymer for pHâ€independent Oxygen Sensing. Electroanalysis, 2015, 27, 2745-2752.	2.9	3
367	High-quality graphene grown on polycrystalline PtRh20 alloy foils by low pressure chemical vapor deposition and its electrical transport properties. Applied Physics Letters, 2016, 108, .	3.3	3
368	Integrated Methylome and Transcriptome Analysis Provides Insights into the DNA Methylation Underlying the Mechanism of Cytoplasmic Male Sterility in Kenaf (Hibiscus cannabinus L.). International Journal of Molecular Sciences, 2022, 23, 6864.	4.1	3
369	The synergistic effect supported Li 4 Ti 5 O 12 anode with advanced lithium storage performance. Materials Chemistry and Physics, 2017, 201, 362-371.	4.0	2
370	Patterned optical anisotropic film for generation of non-diffracting vortex beams. Applied Physics Letters, 2022, 120, .	3.3	2
371	Fabrication of all-in-one multifunctional phage liquid crystalline fibers. RSC Advances, 2013, 3, 20437.	3.6	1
372	Parallel Processing OAM Modes Through Liquid Crystal Photoalignment. , 2018, , .		1
373	An All-Liquid-Crystal Strategy for Fast Orbital Angular Momentum Encoding and Optical Vortex Steering. IEEE Journal of Selected Topics in Quantum Electronics, 2022, 28, 1-6.	2.9	1
374	Bandâ€Gap Manipulations of Monolayer Graphene by Phenyl Radical Adsorptions: A Density Functional Theory Study. ChemPhysChem, 2014, 15, 2610-2617.	2.1	0
375	Superstructures: Smectic Layer Origami via Preprogrammed Photoalignment (Adv. Mater. 15/2017). Advanced Materials, 2017, 29, .	21.0	0
376	Generations of multiple orbital angular momentum modes in 2D nonlinear photonic crystal. , 2017, , .		0
377	Visible and Online Detection of Nearâ€Infrared Optical Vortices via Nonlinear Photonic Crystals (Advanced Optical Materials 1/2022). Advanced Optical Materials, 2022, 10, .	7.3	0